Available online at www.sciencedirect.com
SCIENCE DIRECT®
Journal of Catalysis 221 (2004) 170–177
JOURNAL OF CATALYSIS
www.elsevier.com/locate/jcat

Different modification effects of carbidic and graphitic carbon on Ni surfaces

Henry H. Hwu,[a,1] Bernd Fruhberger,[c] and Jingguang G. Chen [a,b,*]

[a] *Department of Materials Science and Engineering, Center for Catalytic Science and Technology, University of Delaware, Newark, DE 19716, USA*
[b] *Department of Chemical Engineering, Center for Catalytic Science and Technology, University of Delaware, Newark, DE 19716, USA*
[c] *Department of Physics, University of California at San Diego, La Jolla, CA 92093, USA*

Received 12 May 2003; revised 4 August 2003; accepted 5 August 2003

Abstract

The dehydrogenation of cyclohexene was used as a probe reaction to examine the effect of carbide and graphite modifications on Ni surfaces. The carbon-modified surfaces were first characterized with Auger electron spectroscopy (AES) and near edge X-ray absorption fine structure (NEXAFS), where the transformation from carbidic to graphitic carbon was detected after heating the carbon overlayer to 900 K. The reaction pathways of cyclohexene on the modified Ni surfaces were then compared with those on the unmodified Ni surface using temperature-programmed desorption (TPD) and high-resolution electron energy loss spectroscopy (HREELS). Thermal desorption studies showed that on the clean Ni surface, 39% of the adsorbed cyclohexene underwent dehydrogenation to benzene, while the remaining 61% completely decomposed to surface carbon and gas-phase hydrogen. The formation of carbide significantly modified the surface chemistry of Ni. For example, upon carbide modification, the selectivity toward benzene increased to 79%. After converting the carbide to graphite, the overall surface activity was reduced by a factor of 2.2, but the selectivity toward benzene remained at 79%. Vibrational studies further revealed that cyclohexene was converted to benzene by 200 K on the modified and unmodified Ni surfaces, and that the degree of interaction was different between benzene and the three surfaces.

Keywords: Ni carbides; Ni; Graphitic carbon; HREELS; NEXAFS

1. Introduction

Nickel-based catalysts are an integral part of the industrially important steam reforming and methanation processes [1–3]. When these reactions are operated under the most economical conditions, the presence of carbonaceous materials on Ni is unavoidable [3]. As a result, the desire to understand the effect of carbon on the catalytic activity has led to a variety of experimental and theoretical investigations [2–7]. A few select studies are briefly described below. Goodman and co-workers used Auger analysis to identify two types of carbon species after the reactions of carbon monoxide and ethylene on Ni(100) at 600 K [4,5]. Blakely and co-workers examined carbon coverages as a function of temperature on Ni(111) and detected the formation of a graphite monolayer on Ni(111) at temperatures below 1080 K [6]. Broadbelt and co-workers further expanded the database of geometric and energy parameters of this system by using density functional theory to calculate the binding energy and bond lengths of atomic carbon on Ni(111) [2]. Norskov and co-workers combined a variety of modeling results with thermogravimetric analysis (TGA) and extended X-ray absorption spectroscopy (EXAFS) data to detail the interaction of carbon and Ni(111) in the steam reforming process [3]. In summary, carbon species on Ni catalyst are characterized as either carbidic or graphitic, with the carbidic form resulting in useful hydrocarbon product and the graphitic form leading to catalyst deactivation [2,4,5].

In general, Ni surfaces containing carbidic or graphitic carbon can be prepared through the decomposition of carbon monoxide ($2CO_{(g)} \rightarrow C_{(ad)} + CO_{2(g)}$) or ethylene ($C_2H_{4(g)} \rightarrow 2C_{(ad)} + 2H_{2(g)}$). Various groups have studied the formation of carbidic carbon on single crystal Ni surfaces [7–11]. McCarty and Madix studied the reactions of CO, CO_2, H_2, H_2O, and formic acid on Ni(110)–(4×5)C and

* Corresponding author.
E-mail address: jgchen@udel.edu (J.G. Chen).
[1] Present address: Institute of Bioengineering and Nanotechnology, SI Science Park Road, Singapore Science Park II, Republic of Singapore 117586.

0021-9517/$ – see front matter © 2003 Published by Elsevier Inc.
doi:10.1016/j.jcat.2003.08.003

Ni(110)–graphite surfaces [7,8]. Nakamura and co-workers showed that the growth mode of carbide islands on Ni(111) was different depending on whether CO or ethylene was used [9]. Regardless of the Ni surfaces examined and the techniques used, the one commonality in these investigations was that the carbides were prepared at an intermediate temperature between 400 and 600 K; the graphitized surfaces were obtained by heating the carbide layers to 700 K and above [7–11].

Our group has reported extensively the effect of carbon modification on group IV–VI early transition metals toward the reaction of hydrocarbon molecules [12–20]. Specifically, these studies demonstrated that these transition metal carbides (TMC) often exhibit reaction pathways that are similar to those of the Pt group metals. We have used the dehydrogenation of cyclohexene to benzene as a probe reaction to compare the catalytic activity of carbide-modified Mo(110) [14,15], W(111) [16], V(110) [17], and Ti(0001) [18] to that of Pt(111) [19]. One of the objectives of the study is to examine the effect of carbide modification on a late transition metal such as Ni.

The manuscript is organized as follows: We will first present the characterization of carbide- and graphite-modified Ni surfaces by Auger electron spectroscopy (AES) and near edge X-ray absorption fine structure (NEXAFS). We will then use the thermal desorption and vibrational studies of adsorbed cyclohexene to demonstrate the different modification effects of carbidic and graphitic carbon on Ni surfaces.

2. Experimental

2.1. Techniques

Two ultrahigh vacuum (UHV) chambers were used in this study, and were both described in earlier publications [20–22]. The AES, temperature-programmed desorption (TPD), and high-resolution electron energy loss spectroscopy (HREELS) experiments were conducted using a chamber at the University of Delaware. Briefly, it is a three-level chamber that is equipped with a double-pass cylindrical mirror analyzer for AES, a quadrupole mass spectrometer (UTi) for TPD measurements, and an LK-3000 HREEL spectrometer. The HREEL spectra reported here were acquired with a primary beam energy of 6.0 eV. Count rates for the elastic peak were typically in the range from 5×10^5 to 1.0×10^6 counts per second, and the spectral resolution was between 24 and 36 cm^{-1}. For TPD and HREELS experiments, the cyclohexene exposures were made at 80 K and the surfaces were heated with a linear heating rate of 3 K/s.

The carbon *K*-edge NEXAFS spectra were measured in a second chamber at the National Synchrotron Light Source (NSLS), Brookhaven National Laboratory (ExxonMobil U1A beamline). The beamline instrumentation has been described in detail previously [21]. In addition, the UHV chamber was equipped with AES and TPD to ensure identical chamber and surface conditions at both experiment locations. The NEXAFS spectra were recorded by measuring partial electron yield using a channeltron multiplier located near the sample surface.

Cyclohexene (Aldrich, 99.99% purity) was purified by several freeze-pump-thaw cycles prior to use. All other gases (oxygen and neon) used were of research purity and were introduced into the UHV chamber without further purification. The purity of all gases was verified by in situ mass spectrometry. Gas exposures were reported in Langmuirs ($1.0\ L = 1.0 \times 10^{-6}$ Torr s) and were not corrected for differences in gas ionization probabilities.

2.2. Surface preparations

The main advantage of preparing epitaxial Ni(111) films on Pt(111), rather than using a Ni(111) single crystal, was that it allowed for the direct comparison of experimental results between carbon-modified surfaces and Pt(111) under identical conditions. Epitaxial Ni(111) films were prepared by evaporating Ni onto a clean Pt(111) surface. The Pt(111) crystal (1.5 mm thick, 12 mm diameter, 99.999% pure) was purchased from Metal Crystal & Oxide Ltd., and was mounted to the manipulator by spotwelding directly to two Ta posts. The sample temperature was measured by spot welding a type K thermocouple to the back of the Pt(111) crystal. Clean and well-ordered Pt(111) surfaces were obtained by Ne^+ bombardment at 900 K (3 kV, ~ 6 μA sample current) followed by annealing at 1100 K, and by oxygen treatment, as described previously [22]. During metal deposition, the Pt(111) surface was held at 600 K to prevent CO adsorption. The Ni source consisted of a Ni wire (99.999% purity) wrapped around a resistively heated tungsten wire, which was contained in a stainless-steel enclosure with an opening approximately 1 cm in diameter. The concentration of impurities (mainly carbon) on the Ni(111) films was just at or below the AES detection limits. At 600 K, Ni grows epitaxially on Pt(111), leading to the formation of a Ni film with a sharp (111) LEED pattern at higher Ni coverages [22]. The Ni/Pt(111) surfaces used in the current study did not show any Pt Auger transition at 237 eV from the Pt(111) substrate, indicating that the Ni(111) films were at least 20 Å in thickness. Furthermore, AES analysis after the reaction of cyclohexene, at temperatures up to 600 K, did not detect any Auger peaks from the Pt substrate, suggesting that the Pt(111) substrate remained covered by the Ni film.

3. Results and interpretation

3.1. Converting carbidic to graphitic carbon on Ni surfaces

The preparation of the carbide-modified Ni/Pt(111) surface, or C/Ni/Pt(111), began by first preparing a Ni(111) film at 600 K. The Ni/Pt(111) surface was then exposed to one to

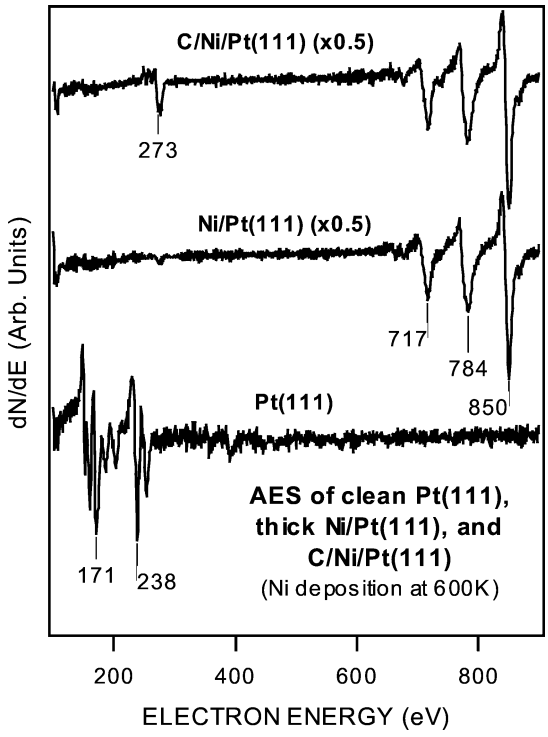

Fig. 1. Auger spectra of clean Pt(111), Ni/Pt(111), and 1-cycle C/Ni/Pt(111).

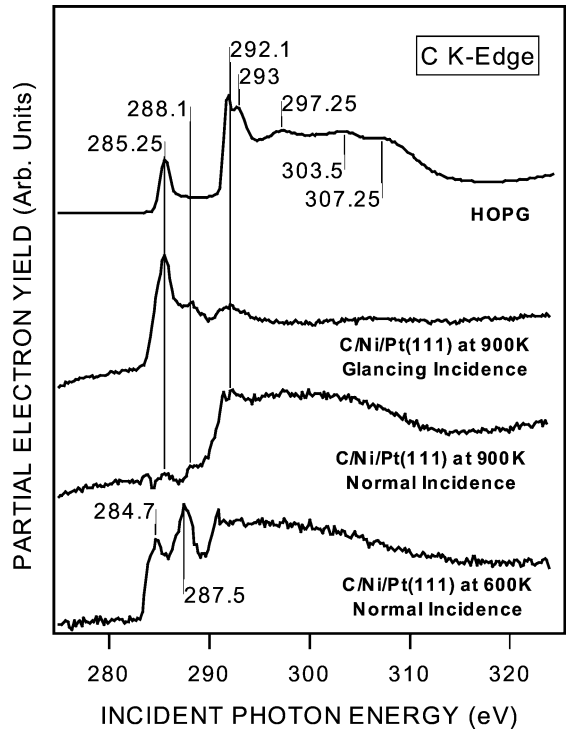

Fig. 2. C K-edge NEXAFS spectra illustrating the temperature and polarization dependence of the C/Ni/Pt(111) surface.

three saturation (3.0 L) cycles of cyclohexene at 80 K, followed by heating to 600 K. Typically, the AES peak-to-peak ratios of C(KLL 273 eV)/Ni(LMM 850 eV) after cyclohexene exposures were $\sim$0.25 (1 cycle), $\sim$0.40 (2 cycle), and $\sim$0.60 (3 cycle). Fig. 1 compares the Auger spectra of Pt(111), Ni(111) film, and 1-cycle C/Ni/Pt(111). These measurements revealed that the Pt(111) substrate was completely buried by the Ni overlayer, as evident by the absence of any Pt Auger transitions on the Ni(111) film and C/Ni/Pt(111) surfaces.

NEXAFS measurements were performed to differentiate the carbidic and graphitic nature of the carbon atoms on the modified Ni/Pt(111) surfaces Fig. 2 compares the carbon K-edge NEXAFS features of the two surfaces. The C/Ni/Pt(111) surface has the characteristic C K-edge features of transition metal carbides [23–25] at $\sim$284.7 and 287.5 eV, which disappear after the surface is heated to 900 K to form graphite/Ni/Pt(111). The middle two spectra in Fig. 2 were recorded with the angles of the incident photons at normal and 25° glancing with respect to the Ni(111) film. The overall C K-edge features in the two spectra are similar to those of the highly oriented pyrolitic graphite (HOPG), which is represented by the top spectrum [26]. One important observation is that the intensities of the C K-edge features of graphite on Ni/Pt(111) are dependent on the angles of the incident photons, with the π^* feature at 285.5 eV being very intense at the glancing incidence and the broad σ^* features above 292.1 eV being more intense at the normal incidence. Such an angular dependence suggests that the carbidic carbon atoms on Ni/Pt(111) are converted to graphite-like structures at 900 K, and that the basal plane of the graphite is parallel to the Ni/Pt(111) surface [27]. Overall, the NEXAFS detection of the thermally induced conversion of carbide to graphite helps to explain the different reactivity of the C/Ni/Pt(111) and graphite/Ni/Pt(111) surfaces, as described in the following sections.

3.2. TPD results

The TPD spectra following the adsorption of 3.0 L of cyclohexene at 80 K on C/Ni/Pt(111) and graphite/Ni/Pt(111) are shown in Fig. 3. For comparison, Fig. 3 also includes the desorption spectra of benzene and hydrogen following the dehydrogenation of cyclohexene on Pt(111) and on an unmodified Ni(111) film. The interaction of cyclohexene on Pt(111) and Ni/Pt(111) has both been discussed in detail previously [28]. For clean Pt(111), H_2 peaks are detected at 301 and 407 K, with an asymmetric benzene desorption at 404 K. The first hydrogen peak at 301 K is most likely attributed to the initial cleaving of C–H bonds to form surface benzene [19,29,30]. The other H_2 peak at 407 K corresponds to the further decomposition of benzene to form surface carbon [19,29,30]. On the Ni(111) film, hydrogen also desorbs at two temperatures as a broad peak at 343 K and a weaker feature at 464 K. The H_2 desorption temperatures and peak shapes deviate slightly from our prior study [28]; these differences can be attributed to variations in the chamber pumping speed and in the location of the crystal surface relative to the mass spectrometer. The overall desorption peak areas, however, are nearly identical to those

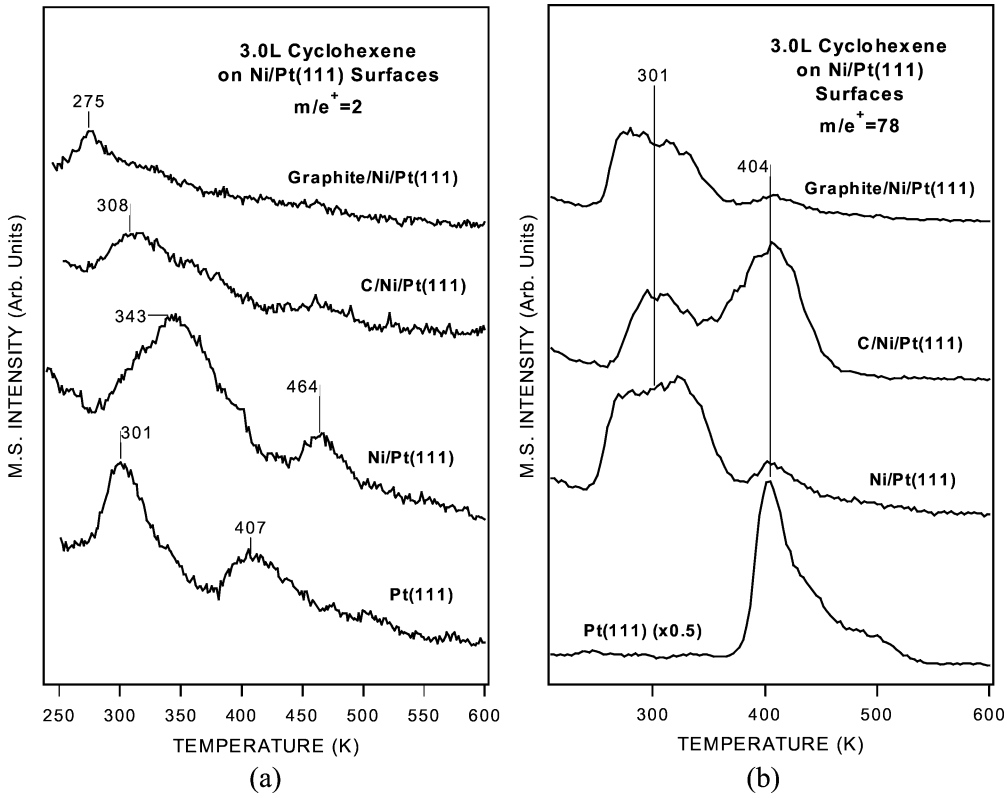

Fig. 3. TPD spectra of (a) hydrogen and (b) benzene obtained following 3.0 L exposures of cyclohexene on clean Pt(111), Ni/Pt(111), C/Ni/Pt(111), and graphite/Ni/Pt(111) at 80 K.

observed previously. Benzene desorption on the Ni(111) film is characterized by a dominant peak centered approximately at 301 K, with a much weaker desorption feature at ∼404 K.

After modifying the Ni/Pt(111) surface by carbide formation, hydrogen desorption is significantly decreased relative to that from Pt(111) or the Ni(111) film. The desorption of the benzene product from C/Ni/Pt(111) appears as two slightly overlapping peaks at 301 and 404 K, with the latter peak being dominant. Interestingly, the 301 K peak coincides with the benzene desorption from the Ni(111) film, while the 404 K feature coincides with the desorption of benzene from Pt(111). On the graphite/Ni/Pt(111) surface, hydrogen desorption is even weaker at 275 K. The benzene desorption peaks on this surface strongly resemble that on the unmodified Ni/Pt(111) surface, but are visibly less intense. These TPD measurements clearly show that carbidic and graphitic carbon atoms modify the surface reactivities of Ni/Pt(111) in a different manner.

To quantify the dehydrogenation activity of cyclohexene on C/Ni/Pt(111) and graphite/Ni/Pt(111), we first performed a mass balance calculation of cyclohexene on the unmodified Ni(111) film. The observed reaction pathways of cyclohexene on the Ni(111) film can be summarized by the following equations

$$x\mathrm{C_6H_{10(a)}} \xrightarrow{\Delta} 6x\mathrm{C_{(a)}} + 5x\mathrm{H_{2(g)}}, \tag{1}$$

$$y\mathrm{C_6H_{10(a)}} \xrightarrow{\Delta} y\mathrm{C_6H_{6(g)}} + 2y\mathrm{H_{2(g)}}. \tag{2}$$

Reaction (1) represents the complete dissociation of cyclohexene, whereas reaction (2) is the dehydrogenation of cyclohexene to produce benzene. The values of x and y were previously obtained to be 0.068 and 0.044 cyclohexene molecules per Ni atom, respectively [28]. The overall activity on the Ni(111) film was therefore $x + y = 0.112$ cyclohexene molecules per Ni atom, with approximately 39% of the cyclohexene dehydrogenating to form gas-phase benzene [28].

In the current study the selectivity values for cyclohexene on the C/Ni/Pt(111) and graphite/Ni/Pt(111) surfaces are determined by comparing their relative hydrogen and benzene desorption peak areas to those from the unmodified Ni/Pt(111) surface. Using the relationships shown below, we calculated the values x and y for C/Ni/Pt(111) to be 0.013 and 0.049 molecules per Ni atom, respectively,

$$\frac{\mathrm{Area}_{\mathrm{Benzene}}^{\mathrm{C/Ni/Pt(111)}}}{\mathrm{Area}_{\mathrm{Benzene}}^{\mathrm{Ni/Pt(111)}}} = 1.11 \Rightarrow y_{\mathrm{C/Ni/Pt(111)}} = 0.049, \tag{3}$$

$$\frac{\mathrm{Area}_{\mathrm{Hydrogen}}^{\mathrm{C/Ni/Pt(111)}}}{\mathrm{Area}_{\mathrm{Hydrogen}}^{\mathrm{Ni/Pt(111)}}} = 0.38 \Rightarrow (5x + 2y)_{\mathrm{C/Ni/Pt(111)}} = 0.16$$

$$\Rightarrow x = 0.013. \tag{4}$$

The overall activity on C/Ni/Pt(111) is therefore 0.062 cyclohexene molecules per Ni atom, with approximately 79% of the cyclohexene dehydrogenating to produce gas-phase benzene. Using identical methods described above,

Table 1
Product yields of cyclohexene on Ni/Pt(111), C/Ni/Pt(111), and graphite/Ni/Pt(111)

Surface	C_6H_6 activity per Ni atom (% selectivity)	Complete decomposition activity per Ni atom (% selectivity)	Overall activity per Ni atom
Ni/Pt(111) [28]	0.044 (39)	0.068 (61)	0.112
C/Ni/Pt(111)	0.049 (79)	0.013 (21)	0.062
Graphite/Ni/Pt(111)	0.022 (79)	0.006 (21)	0.028

Table 2
Vibrational assignments for cyclohexene on Ni/Pt(111), C/Ni/Pt(111), and graphite/Ni/Pt(111)

Mode	Liquid [41]	C_6H_{10} on Ni/Pt(111) [28]	C_6H_{10} on C/Ni/Pt(111)	C_6H_{10} on graphite/Pt(111)
Ring deformation ν(M–C)	175, 280, 393, 452			
Skeletal distortion	640, 670	642	649	643
δ(C=C)	720	724	731	717
ν(C–C)	810, 905, 917	805, 913	819, 913	805, 900
ν(C–C) + $\rho(CH_2)$	1038	1021	1055	1028
$\omega(CH_2)$ rock	1138	1143	1143	1130
$\omega(CH_2)$ twist	1241, 1264	1251	1258	1245
$\omega(CH_2)$ wag	1321–1350	1346	1353	1333
$\delta(CH_2)$ scissors	1438–1456	1448	1454	1434
ν(C=C)	1653			
ν(–C–H)	2840–2993	2908	2922	2909
ν(=C–H)	3026, 3065			

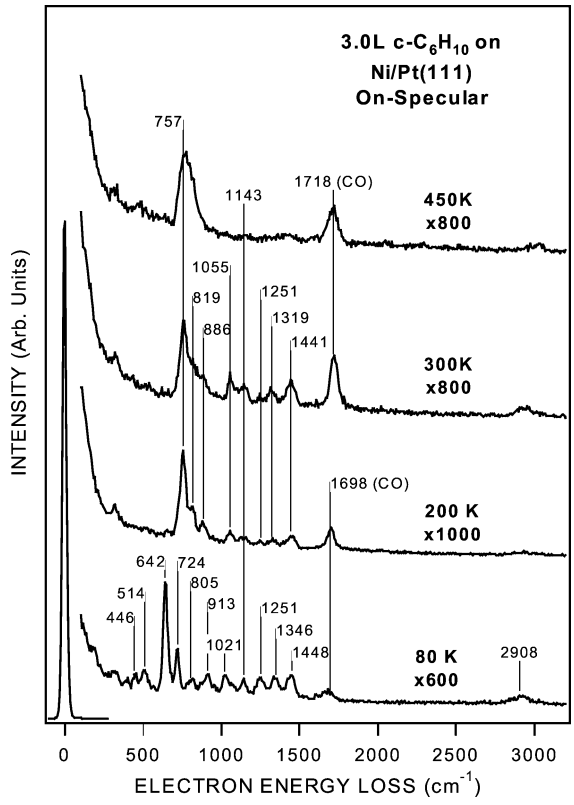

Fig. 4. On-specular HREEL spectra monitoring the thermal decomposition of 3.0 L of cyclohexene on Ni/Pt(111) following adsorption at 80 K.

the values of x and y for the graphite/Ni/Pt(111) surface are calculated to be 0.006 and 0.022 cyclohexene molecules per Ni atom, corresponding to an overall activity of 0.028. The surface reactivity of C/Ni/Pt(111) toward cyclohexene is reduced by a factor of 2.2 when heated to form graphite/Ni/Pt(111). A summary of the cyclohexene activity and product selectivity is provided in Table 1.

3.3. HREEL studies

HREEL spectra for cyclohexene adsorbed on Ni/Pt(111), C/Ni/Pt(111), and graphite/Ni/Pt(111) are described in this section. The exposures of c-C_6H_{10} were made with the crystal temperature at 80 K. The thermal properties of the adsorbed layers were monitored by heating to the temperatures indicated on the figures and cooled immediately before the spectra were recorded. The elastic peaks in all spectra have been normalized to unity, and the expansion factor for each individual spectrum represents the multiplication factor relative to the elastic peak. The mode assignments for molecular cyclohexene on the various surfaces are summarized in Table 2.

3.3.1. Cyclohexene on Ni/Pt(111)

To provide a basis for comparison, we will first assign the vibrational modes of cyclohexene adsorbed on the unmodified Ni/Pt(111) surface. Fig. 4 shows the HREEL spectra recorded after exposing the Ni(111) film to 3.0 L of cyclohexene at 80 K. At 80 K, the detection of the characteristic skeletal distortion mode at 642 cm^{-1}, the δ(C=C) mode at 724 cm^{-1}, and the ν(C=C) mode at 1684 cm^{-1} [16] indicates that molecular cyclohexene species are still intact. After heating to 200 K, however, the spectroscopic changes are consistent with the conversion of cyclohexene to benzene. Specifically, the intense mode at 757 cm^{-1} and the weaker feature at 819 cm^{-1} are characteristic of benzene on Ni(111) surfaces [31]. Using the Herzberg notation [32], the 757 and 819 cm^{-1} modes are ascribed to the ν_4 and ν_{11} modes of benzene, respectively, which are concerted out-of-plane deformations of the C–H bonds. Further heating to 300 K results in the broadening of the 757 cm^{-1} peak. The near absence of the ν(CH) modes indicates that the benzene ring is approximately parallel to the surface, which corresponds well with prior investigations on Ni(111) single crystals [31,33]. Together with the TPD results (Fig. 3), we conclude that the evolution of benzene from the Ni(111) film is desorption limited. At 450 K, only the γ(C–H) (764 cm^{-1}) and the background CO contamination (1711 cm^{-1}) features remain on the surface. The mode assignments for free and adsorbed benzene are provided in Table 3.

3.3.2. Cyclohexene on C/Ni/Pt(111) and graphite/Ni/Pt(111)

When cyclohexene is exposed to the C/Ni/Pt(111) surface, the eventual product is also benzene, but there appear

Table 3
Vibrational assignments for chemisorbed benzene on Ni(111), Ni/Pt(111), C/Ni/Pt(111), and graphite/Ni/Pt(111) film

Mode	Free benzene [42]	Chemisorbed C_6H_6 on Ni(111) [33]	Ni/Pt(111) [28]	C/Ni/ Pt(111	graphite/ Ni/Pt(111)
ν(M–C)					
γ(C–H)	673, 845	745	757, 819	731	744, 798
ν(C–C)	993	845	886	879	
δ(C–H)	1038, 1150	1110	1055, 1143		
δ(C–C)	1309	1320	1333		
ν(C–C) + δ(C–C)	1486	1420	1441	1448	
ν(C–C)	1596				
ν(C–H)	3074	3020			

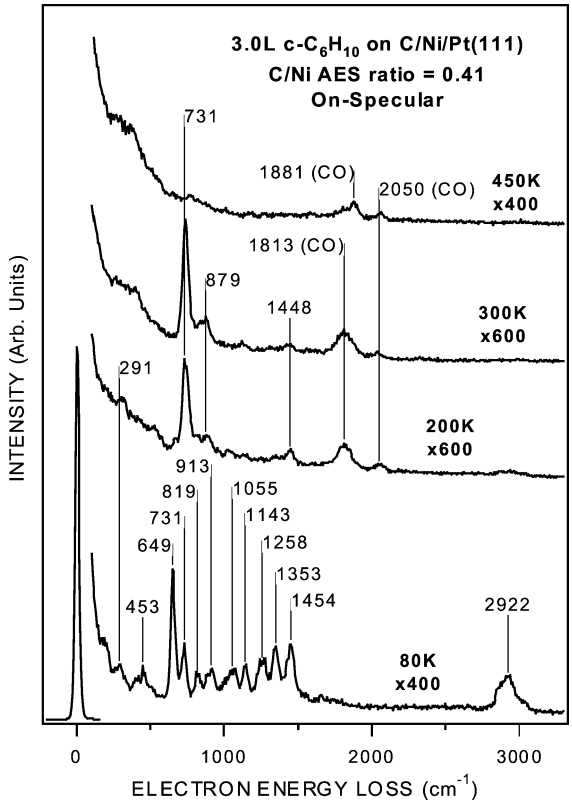

Fig. 5. On-specular HREEL spectra monitoring the thermal decomposition of 3.0 L of cyclohexene on C/Ni/Pt(111) following adsorption at 80 K.

to be two different reaction pathways, as evidenced by the observation of benzene desorption at 301 and 404 K. Fig. 5 shows HREEL spectra recorded after exposing C/Ni/Pt(111) to 3.0 L of cyclohexene at 80 K, and then heating to the indicated temperatures. At 80 K, the presence of the characteristic skeletal distortion mode at 649 cm^{-1} and the δ(C=C) mode at 731 cm^{-1} [28] indicates that molecular cyclohexene species are still intact. The lower frequency peaks at 291 and 453 cm^{-1} are most likely associated with Ni–C vibrations. After heating to 200 K, significant changes in the spectrum are consistent with the conversion of cyclohexene to benzene. Specifically, the intense mode at 731 cm^{-1} and the

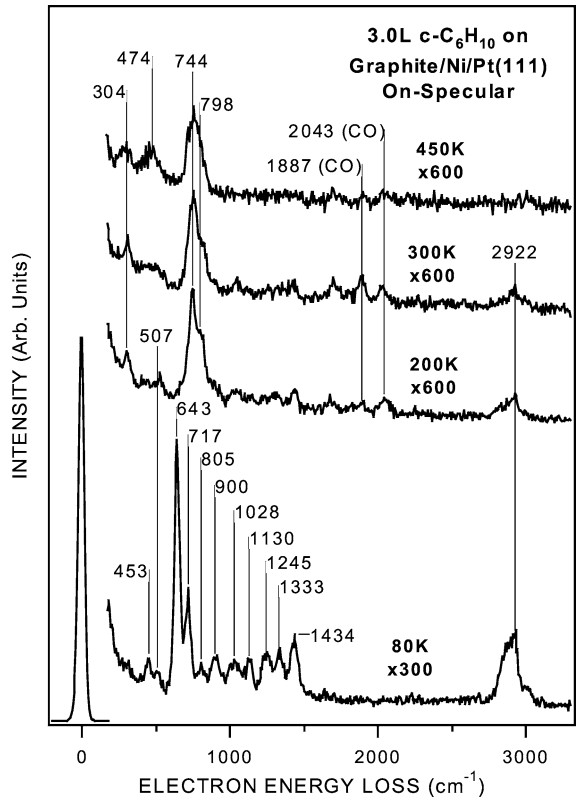

Fig. 6. On-specular HREEL spectra monitoring the thermal decomposition of 3.0 L of cyclohexene on graphite/Ni/Pt(111) following adsorption at 80 K.

shoulder at 879 cm^{-1} are assigned to the ν_4 and ν_{11} mode of benzene, respectively. Additionally, the complete absence of ν(CH) modes indicates that the benzene ring is also lying nearly flat on this surface. Further heating to 300 K resulted in the 731 cm^{-1} peak becoming more intense. This is in contrast to the 300 K spectra on the Ni(111) film, where we observed significant peak broadening of the same mode. The fact that the 731 cm^{-1} peak on C/Ni/Pt(111) remains very sharp indicates that most of the benzene interacts relatively weakly with the surface.

Lastly, the 450 K spectrum shows only a small CO contamination peak near 1900 cm^{-1}. The combination of HREELS and TPD results (Fig. 3) suggests the following reaction sequence on C/Ni/Pt(111): (1) cyclohexene dehydrogenates to benzene by 200 K, (2) hydrogen desorbs at $\sim$300 K, but benzene remains until above 300 K, and (3) the evolution of benzene is desorption limited.

Fig. 6 shows HREEL spectra following the thermal behavior of 3.0 L of cyclohexene on the graphite/Ni/Pt(111) surface. The spectrum at 80 K is similar to that of C/Ni/Pt(111), with characteristic skeletal deformation and δ(C=C) modes at 649 and 724 cm^{-1}, respectively. As before, these features are indicative of molecularly adsorbed cyclohexene [28]. Further heating to 200 and 300 K results in the disappearance of all cyclohexene features. The only remaining vibrational modes are at 304, 507, 744, and 2909 cm^{-1}, which can be assigned as adsorbed benzene. At 450 K, small

changes are observed as the CH_x mode at 2909 cm^{-1} disappears and an additional Ni–C mode at 474 cm^{-1} appears.

4. Discussion

4.1. Different modification effects of carbidic and graphitic carbon

The comparison of the HREELS results indicates that, although benzene is produced on unmodified Ni/Pt(111), C/Ni/Pt(111), and graphite/Ni/Pt(111) by 200 K, the bonding of benzene is different on the three surfaces. This is indicated by the different frequencies and lineshapes of the γ(C–H) modes at 757 and 819 cm^{-1} on the Ni(111) film, at 731 and 879 cm^{-1} on C/Ni/Pt(111), and at 744 and 819 cm^{-1} on graphite/Ni/Pt(111). The different binding strengths of benzene are most likely responsible for the different desorption temperature and product selectivity of gas-phase benzene observed in the TPD measurements.

The C/Ni/Pt(111) surface is significantly different from unmodified Ni/Pt(111) in terms of benzene desorption temperature, benzene selectivity, and the bonding environment of the benzene intermediate. As pointed out by Grassian and Muetterties [34] and Eng et al. [35], the strength of benzene–metal interaction is qualitatively related to the frequency of the ν_4 out-of-plane mode, with the lower frequencies corresponding to weaker interactions. Using a similar correlation, the HREELS results presented above suggest that the benzene intermediate interacts more strongly on the Ni(111) film (757 cm^{-1}) than on C/Ni/Pt(111) (731 cm^{-1}). The stronger bond on the unmodified Ni/Pt(111) surface should be responsible for the relative facile decomposition of the benzene intermediate. Such comparison indicates that the chemical properties of Ni can be modified by the formation of carbide. It is interesting to point out the strong similarities between C/Ni/Pt(111) and Pt(111) in both the benzene selectivity (79% versus 75%, respectively) and benzene desorption temperature (dominant peaks at 404 K).

The interpretation of the HREELS results on graphite/Ni/Pt(111) is less straightforward, because the ν_4 and ν_{11} modes appear to overlap at 200 K and above. Although the frequencies are in the region expected for adsorbed benzene, the relative intensities of these two features are somewhat altered. More detailed vibrational studies are necessary to determine the exact nature of the surface intermediates on graphite/Ni/Pt(111) in the temperature range of 200 and 450 K.

Based on the general similarity in the benzene TPD spectra of unmodified Ni/Pt(111) and graphite/Ni/Pt(111), one may speculate that the C/Ni/Pt(111) surface, when heated to 900 K, segregates into regions of graphite and regions of exposed Ni. The differences in the HREEL spectra and in the hydrogen desorption temperatures, however, argue against such a model. The different selectivity toward gas-phase benzene, 39% on the Ni(111) film and 79% on graphite/Ni/Pt(111), further supports the likelihood that graphite/Ni/Pt(111) is chemically different from unmodified Ni/Pt(111).

McCarty and Madix have reported the adsorption of CO, H_2, H_2O, and DCOOH on clean, carbide- and graphite-modified Ni(110) [7,8]. They reported that the presence of surface carbide significantly reduced the chemisorption ability of Ni(110). Moreover, upon the formation of a graphitic overlayer by heating the carbide surface to $\sim$800 K, the surface was no longer capable of significant chemisorption [7,8]. Similar observations detailing the role of graphitic carbon as site blockers have also been reported for Ru [36] and Pt [37,38] surfaces.

The results presented in the current paper clearly confirmed the different modification effects on carbidic and graphitic carbon on the chemical properties of Ni surfaces. The formation of the graphite on Ni/Pt(111) leads to a significant reduction, although not the complete inhibition, of the chemisorption ability and subsequent reaction of cyclohexene. Therefore the modification effect of graphitic carbon is primarily the site-blocking effect. On the other hand, the presence of carbidic carbon on Ni significantly modifies the reaction pathway and product selectivity. As described in Section 4.2, such a modification effect on Ni is very similar to the observed on carbide-modified early transition metal surfaces. The effect of carbidic carbon on early transition metals has been generally accepted as a modification of the electronic properties [12]. Using the same analogy, we suggest that the modification effect of carbidic carbon on Ni is most likely by electronic modification.

4.2. Brief comparisons with early transition metal carbides

Our group had previously reported the dehydrogenation of cyclohexene to benzene on several carbide-modified early transition metal surfaces [12,14–16,18]. The current study shows that on a late transition metal such as Ni, carbide modification can also modify its surface reactivity to be highly selective toward the formation of gas-phase benzene, similar to that observed on C/Mo(110) [14,15], C/W(111) [16], and C/Ti(0001) [18]; however, upon closer examination of the TPD and HREELS results, one can identify several important differences between the carbide-modified surfaces of early and late transition metals.

On C/Mo(110), C/W(111), and C/Ti(0001), the benzene desorption is generally characterized by a single asymmetric peak between 260 and 330 K [14–16,18]. On C/Ni/Pt(111), however, two benzene desorption states were observed at 301 and 404 K (Fig. 4). The existence of multiple benzene peaks suggests that carbide modification on Ni/Pt(111) may be less uniform than that on early transition metal surfaces. Additionally, HREEL spectra clearly show the presence of adsorbed benzene on C/Ni/Pt(111) by 200 K. The combination of vibrational and thermal desorption results leads one to conclude that the evolution of benzene is desorption limited. This is in contrast to the reaction limited evolution of

gas-phase benzene on the carbide-modified early transition metal surfaces [14–16,18].

Another important difference between early and late transition metals is the thermal stability of carbidic carbon. Generally, carbidic carbon on early transition metal surfaces either diffuses into the bulk [17,18] or migrates to interstitial sites [14–16] at elevated temperatures, instead of converting to graphite. On the other hand, carbidic carbon on Ni/Pt(111) completely converts to graphite when heated to 900 K. The thermal transformation of carbide to graphite has also been predicted and observed on the surfaces of Fe [39], Co [40], and Cu [39]. These results further confirm the different thermal stability of early and late transition metal carbides.

5. Conclusions

Carbidic and graphitic carbon layers have been grown on Ni(111) film by repeated cycles of cyclohexene exposure followed by heating to either 600 or 900 K, respectively. NEXAFS studies have highlighted the differences between carbide and graphite modifications on the Ni/Pt(111) surface. The thermal decomposition of cyclohexene over clean and modified Ni/Pt(111) has also been compared using TPD and HREELS. On the Ni(111) film, approximately 39% of the adsorbed cyclohexene dehydrogenated to produce gas-phase benzene. When the Ni/Pt(111) surface was modified by carbidic carbon, the selectivity toward the benzene production pathway increased to 79%, which was very similar to that observed for cyclohexene on Pt(111). Upon transformation of the carbide layer to graphite, the selectivity toward benzene remained at 79%, although the overall activity was reduced by a factor of 2.2. In Addition, vibrational studies indicated that the evolution of benzene was desorption limited on all surfaces, and that the interaction between adsorbed benzene and the carbide-modified Ni/Pt(111) was the weakest among the examined surfaces.

Acknowledgments

We acknowledge financial support from the Department of Energy, Basic Energy Sciences (Grant DE-FG02-00ER15104). We also thank Dr. J. Eng, Jr., for his assistance in the experiments. One of us (H.H.H.) acknowledges the financial support from the University of Delaware Presidential Fellowship and the American Vacuum Society Graduate Student Fellowship. Last, we are very grateful to Dr. P.A. Stevens and ExxonMobil for providing beamtime at the National Synchrotron Light Source U1A Beamline.

References

[1] J.R. Rostrup-Nielsen, in: J.R. Anderson, M. Boudart (Eds.), Catalysis, Science and Technology, Vol. 5, Springer, Berlin, 1984, Chap. 1.
[2] D.J. Klinke II, S. Wilke, L.J. Broadbelt, J. Catal. 178 (1998) 540.
[3] H.S. Bengaard, et al., J. Catal. 209 (2002) 365.
[4] D.W. Goodman, R.D. Kelley, T.E. Madey, J.M. White, J. Catal. 64 (1980) 479.
[5] R.D. Kelley, D.W. Goodman, Surf. Sci. 123 (1982) L743.
[6] J.C. Shelton, H.R. Patil, J.M. Blakely, Surf. Sci. 43 (1974) 493.
[7] J.G. McCarty, R.J. Madix, Surf. Sci. 54 (1976) 121.
[8] J.G. McCarty, R.J. Madix, Surf. Sci. 54 (1976) 210.
[9] H. Nakano, J. Ogawa, J. Nakamura, Surf. Sci. 514 (2002) 256.
[10] D.E. Gardin, J.D. Batteas, A. Van Hove, G.A. Somorjai, Surf. Sci. 296 (1993) 25.
[11] C. Astaldi, A. Santoni, F. Della Valle, R. Rosei, Surf. Sci. 220 (1989) 322.
[12] J.G. Chen, Chem. Rev. 96 (1996) 1477.
[13] J.G. Chen, B. Fruhberger, J. Eng Jr., B.E. Bent, J. Mol. Catal. A 131 (1998) 285.
[14] J.G. Chen, B. Fruhberger, Surf. Sci. 367 (1996) L102.
[15] J. Eng Jr., B.E. Bent, B. Fruhberger, J.G. Chen, Langmuir 14 (1998) 1301.
[16] N. Liu, S.A. Rykov, H.H. Hwu, M.T. Buelow, J.G. Chen, J. Phys. Chem. B 105 (2001) 3894.
[17] J.G. Chen, M.D. Weisel, Z.M. Liu, J.M. White, J. Am. Chem. Soc. 115 (1993) 8875.
[18] H.H. Hwu, J.G. Chen, 2003, submitted for publication.
[19] J.A. Rodriguez, C.T. Campbell, J. Catal. 115 (1989) 500.
[20] B. Fruhberger, J.G. Chen, J. Am. Chem. Soc. 118 (1996) 11599.
[21] J.G. Chen, Surf. Sci. Rep. 30 (1997) 1.
[22] B. Fruhberger, J. Eng Jr., J.G. Chen, Catal. Lett. 45 (1997) 85.
[23] J.G. Chen, C.M. Kim, B. Fruhberger, B.D. DeVries, M.S. Touvelle, Surf. Sci. 321 (1994) 145.
[24] R. Kapoor, S.T. Oyama, B. Fruhberger, B.D. DeVries, J.G. Chen, Catal. Lett. 34 (1995) 179.
[25] B. Fruhberger, J.G. Chen, J. Eng Jr., B.E. Bent, J. Vac. Sci. Technol. A 14 (1996) 1475.
[26] R.A. Rosenberg, P.J. Love, V. Rehn, Phys. Rev. B 33 (1986) 4034.
[27] J. Stohr, NEXAFS Spectroscopy, in: Springer Series in Surface Science, Vol. 25, Springer, New York, 1992.
[28] H.H. Hwu, J. Eng Jr., J.G. Chen, J. Am. Chem. Soc. 124 (2002) 702.
[29] J.A. Rodriguez, C.T. Campbell, J. Phys. Chem. 93 (1989) 862.
[30] F.C. Henn, et al., J. Phys. Chem. 96 (1992) 5965.
[31] J. Lehwald, H. Ibach, J.E. Demuth, Surf. Sci. 78 (1978) 577.
[32] J.E. Bertie, C.D. Keefe, J. Chem. Phys. 101 (1994) 4610.
[33] J.C. Bertolini, J. Rousseau, Surf. Sci. 89 (1979) 467.
[34] V.H. Grassian, E.L. Muetterties, J. Phys. Chem. 91 (1987) 389.
[35] J. Eng Jr., B.E. Bent, B. Fruhberger, J.G. Chen, J. Phys. Chem. B 101 (1997) 4044.
[36] M.C. Wu, Q. Xu, D.W. Goodman, J. Phys. Chem. 98 (1994) 5104.
[37] T.A. Land, T. Michely, R.J. Behm, J.C. Hemminger, G. Comsa, Surf. Sci. 264 (1992) 261.
[38] R.I. Kvon, S.V. Koscheev, A.I. Boronin, J. Mol. Catal. A 158 (2000) 297.
[39] R.W. Joyner, G.R. Darling, J.B. Pendry, Surf. Sci. 205 (1988) 513.
[40] M. Zonnevylle, J. Geerlings, R. van Santen, Surf. Sci. 240 (1990) 253.
[41] M.A. Newton, C.T. Campbell, Z. Phys. Chem. 198 (1997) 169.
[42] X. Su, K.Y. Kung, J. Lahtinen, Y.R. Shen, G.A. Somorjai, J. Mol. Catal. A 141 (1999) 9.